ISSN 1063-7710, Acoustical Physics, 2014, Vol. 60, No. 5, pp. 555–561. © Pleiades Publishing, Ltd., 2014.

ACOUSTICS OF STRUCTURALLY INHOMOGENEOUS SOLID BODIES. GEOLOGICAL ACOUSTICS

A Unified Model of Hysteresis and Long-Time Relaxation in Heterogeneous Materials[1]

A. V. Lebedev[a] and L. A. Ostrovsky[a, b]

[a] *Institute of Applied Physics, Russian Academy of Sciences, ul. Ulyanova 46, Nizhni Novgorod, 603950 Russia*

[b] *NOAA Earth Science Research Laboratory, 325 Broadway, Boulder, CO 80305 USA*

e-mail: swan@hydro.appl.sci-nnov.ru; lev.a.ostrovsky@noaa.gov

Received January 15, 2014

Abstract—A physical model of stress-strain dynamics and long-time relaxation (slow time) in structured media is proposed. The model is based on the analysis of inter-grain contacts and the resulting surface force potential with a barrier. The result is a unified description of the classical acoustic nonlinearity, stress-strain hysteresis, and logarithmic relaxation law for sound velocity (and, hence, for the frequency of nonlinear resonance in samples of structured materials). Estimates of a characteristic volume of interacting contacts give close values for the variety of consolidated materials. For weak (linear) testing waves, the logarithmic relaxation occurs if a classical quadratic nonlinearity is added to the stress-strain relation.

Keywords: hysteresis, relaxation, slow time, Arrhenius law

DOI: 10.1134/S1063771014050066

INTRODUCTION

Understanding of mechanisms of acoustic nonlinearity in heterogeneous materials has been and remains an object of intensive studies (e.g., [1–5]). It is known for decades that materials with complex structures such as rock and ceramics possess an anomalously strong acoustic nonlinearity. These features are of great importance for description of seismic phenomena including strong earthquakes (e.g. [6, 7]) as well as for damage diagnostics in heterogeneous media (e.g., [8–10]). Two specific features were registered, separately or often together, in most of the experiments: hysteresis in the stress-strain relation and the long-time relaxation (slow time). A review of the results obtained by different groups of researchers can be found in [1, 2]. However, the existing theoretical models of the above features are essentially phenomenological; the Preisach–Mayergoyz (PM) model based on the integral action of phenomenological (rectangular) hysteretic elements connecting pressure (stress) and displacement (strain) is the most widely used (see [2] and references therein). Also for slow dynamics phenomena only phenomenological models were suggested; in particular, a broad spectrum of partial relaxation times in the PM model was considered in [2]. Note that in [11] effects of thermal fluctuations on the PM elements were considered using the Arrhenius model to predict frequency dispersion.

Here, we propose a physical model of a medium in which nonlinear elasticity incorporates both the phenomena of hysteresis and slow time. This model agrees with the majority of experimental data obtained by different research groups [12–18] in what concerns classical nonlinearity, stress-strain hysteresis and the transition between them, as well as the slow time relaxation, including the existence of threshold in the strain level for exciting the latter process.

BACKGROUND

We take into account two types of contact forces acting between structural elements (called grains in a broad sense), namely, elastic force due to the compressibility of grains (a generalization of the Hertz–Mindlin potential), and the adhesion acting at the contacts with variable areas. The relative contribution of these forces at tension depends on the contact thickness. Classical theory of adhesion phenomena was proposed in [19] and is abbreviated as JKR-theory after its authors. As is well-known, the adhesion is caused by surface forces of various nature [20] and the contact area deformation. Two grains can be detached if the load force exceeds a threshold value, which depends on the sizes and material properties of grains; the reverse process occurs at a different load which results in the hysteresis. It was evaluated in [21] where a controlling parameter was derived:

$$\mu = \left(\frac{V_{\min}^2 R}{E^{*2} h_m^3}\right)^{1/3}, \qquad (1)$$

[1] The article is published in the original.

where $V_{\min}$ is the surface density of potential energy and h_m is the adhesion layer thickness in the equilibrium state, $R = (R_1^{-1} + R_2^{-1})^{-1}$ is the equivalent radius of the contact of two bodies having the radii R_1 and R_2, and $E^* = [(1 - \nu_1^2)/E_1 + (1 - \nu_2^2)/E_2]^{-1}$, where $E_{1,2}$ and $\nu_{1,2}$ are the Young moduli and Poisson ratios, respectively, of the grains in contact. The grains can be considered large and deformable if R is large such that $\mu \gg 1$, and small and stiff in the opposite case. In the latter case the attachment and detachment processes are reversible and there is no hysteresis. If, however, $\mu > 0.81$, then the JKR hysteresis takes place [21]. The adhesion hysteresis has been discussed by many authors (see, e.g., [2, 22, 23]). In particular, in [2] the van der Waals potential at a contact was discussed in detail. For micro-damaged materials, the JKR approach was applied in [24] where the resulting adhesion hysteresis in a microcrack is approximated by a rectangular loop; the ensemble of such contacts is then treated as in the PM model.

In the theory developed here we consider the following processes: (1) the elastic modulus and small quadratic nonlinearity are due to the grains' material compressibility and are defined by the vicinity of the main potential minimum, (2) as was mentioned, the adhesive contact can be broken and then be recovered with a different strain value which creates hysteresis, and (3) besides the main potential minimum defining the linear elastic modulus and classical nonlinearity, there is at least one shallow, metastable minimum of the contact potential energy (e.g., [20, 25]) in which part of the broken contacts remain trapped after the break so that their restoration occurs only due to thermal motion, which needs a prolonged relaxation period (slow time). Integrating the contributions of individual contacts with different curvature radii results in the stress-strain relation which incorporates both classical and hysteretic nonlinearities, as well as long-time relaxation, within the framework of the same contact model. The data confirming that the corresponding contact properties are relevant to rock and other heterogeneous materials can be found in [12–18].

For the adhesive contact force, we use the JKR formula [26]:

$$F = \frac{4E^*a^3}{3R} - \sqrt{8\pi\gamma E^* a^3}, \qquad \delta = \frac{a^2}{R} - \frac{2}{3}\sqrt{\frac{9\pi\gamma a}{2E^*}}, \tag{2}$$

where a is the contact radius, δ is the indentation depth, and γ is the adhesion coefficient, which is equal to $V_{\min}$ specified above if the adhesion layer thickness is not varied (one can easily show this is correct for $m \gg 1$). The contact strength (bond strength) F_c is proportional to R and equal to (see Fig. 2 below)

$$F_c = \pi\gamma R\begin{cases} -\frac{3}{2}, \text{ for detaching at } \delta_c, \\ -\frac{5}{6}, \text{ for detaching at } \delta_c^*. \end{cases} \tag{3}$$

Note that R can significantly exceed the mean grain radius R_g since the contact area is flattened due to the action of high pressure and temperature during the material creation [27]. In particular, glass-like structures found in the contact area [27] point to very smooth surfaces where adhesion effects should be pronounced. The relation between force and displacement can be found from (2) if the minimal surface energy per unit area of a contact is known ($\gamma = V_{\min}$).

For that, however, a more detailed analysis of the adhesive forces has to be made. According to Israelashvili [20], the adhesion potential can be described as follows:

$$V(h) = -\frac{A}{12\pi h^2}\left[1 - \left(\frac{h_0}{h}\right)^6\right] + QkT\exp(-\kappa h), \tag{4}$$

where h is the separation distance between the interacting surfaces, $A = 10^{-20}$–10^{-19} J is the Hamacker constant, $k = 1.38 \times 10^{-23}$ J/K is the Boltzmann constant, T is absolute temperature, and $h_0 \approx 0.1$ nm is the characteristic atomic size. The second term in square brackets describes strong repulsion of atoms (see [20] for details). The factor Q in the last term of (4) depends on the concentration of ions, surface charge density, and other factors [20], and $\kappa = 1/\lambda_D$, where λ_D is the Debye length.

Near the main minimum, the second term in (4) is negligible, and the first term defines the potential minimum; using the latter in (2), the full potential can be found. Note that in this area the parameter μ is large, and h is practically unchangeable (stiff adhesion layer). Under the tension load, μ decreases up to the contact breaking resulting in hysteresis as described above. With a still larger separation of grains, the second term in (4) becomes important; it defines the second, weak potential minimum. An example of the resulting potential is shown in Fig. 1 for quartz grains of equal radii $R_g = 100$ μm at $\gamma = 0.1$ J/m^2. The plot shown in the inset corresponds to $Q = 1.4 \times 10^{18}$ m^{-2}. In this case, there exists a transition into the secondary minimum after the contact is detached. In the secondary minimum, $\mu < 1$, so that there is no JKR-type hysteresis, whereas the slow time relaxation is present.

MACROSCOPIC STRESS-STRAIN HYSTERESIS

Consider now the resulting macroscopic properties of the material in terms of the stress-strain dependence. For small strains, the so-called classical elasticity case (e.g., [1, 2]) takes place. Near the main minimum, Taylor expansion of the total energy yields $U_\Sigma \approx U_{\min} + \alpha(x - x_0)^2 - \beta(x - x_0)^3$, where $x = \delta - h$ is the total displacement (see Fig. 1) and $x_0 = \delta_0 - h_0$ corre-

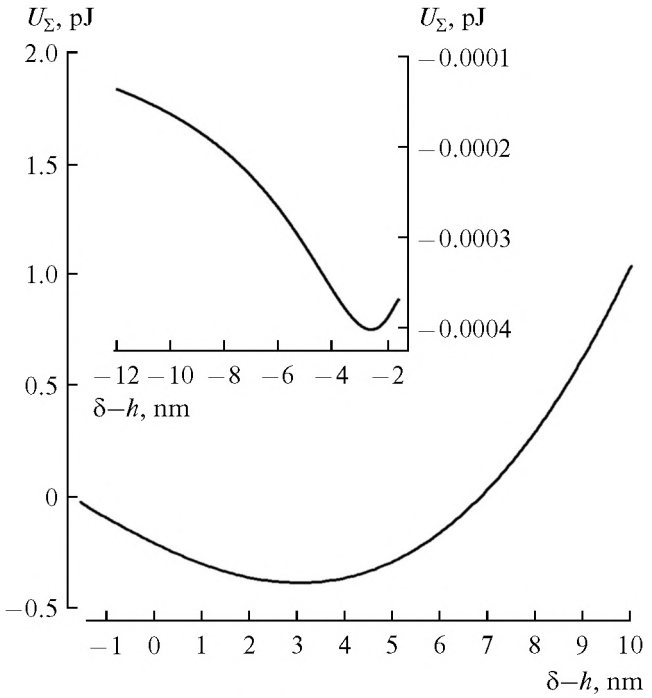

Fig. 1. Contact potential in the vicinity of the main minimum. The positive values of the total displacement correspond to compression, and negative ones—to tension. In the inset the potential at larger distances (detached contact) is shown. See details in the text.

sponds to the main equilibrium position when $F = 0$ in (2). Coefficients α and β can be found by differentiating the function of the type shown in Fig. 1. Macroscopic values of elasticity moduli and the nonlinear parameter can be determined after integrating over the contact radii distribution. The corresponding value of the macroscopic bulk stiffness modulus can be estimated as several GPa for quartz grains with an average curvature radius $R \approx 1$ mm that corresponds to the flattened contact areas [27]. A typical value of the nonlinear parameter $\Gamma_2 = -3\beta R/2\alpha \sim -10^4$ for these grains. These estimates are in good agreement with numerous experimental results for the vibro-acoustic properties of rocks (see, e.g., [1, 2, 13]).

With some negative displacement ($\delta_c \approx -1.7$ in Fig. 1), the adhesion contact breaks. This point corresponds to the detaching force (contact strength defined above) proportional to R. The detaching point can be seen in Fig. 2 where the function $\tilde{\sigma}_h = F/4\pi R_g^2$ is plotted versus $\varepsilon = \delta/2R_g$. Indeed, at some point slow motion along the analytical curve becomes impossible (quadratic form of potential energy becomes non-positive [19]) and for a zero viscosity, a fast "jump" is inevitable. With zero friction, this occurs at $\varepsilon = \varepsilon_c$ where the differential stiffness turns to zero (cf. [22, 23]), whereas at a relatively large viscosity the fast motion starts at $\varepsilon = \varepsilon_c^*$ where $d\sigma/d\varepsilon \to -\infty$ and viscosity cannot prevent the detachment. In [24], fast motion is approximated by a rectangular loop of a PM type. Strictly speaking, it is necessary to consider the transient process taking viscosity and mass into account, and in general the real motion occurs between the two possible jump points mentioned above. In both cases the resulting force turns to zero (broken contact) and then the system returns to the regular curve. To be definite, we have considered the jump at $\varepsilon = \varepsilon_c^*$ which corresponds to the high viscosity associated with the detaching process (e.g., [25]). Note also that the loops shown in Fig. 2 can be considered as physical hysteretic elements instead of the phenomenological rectangular PM loops used before [2].

Consider now the macroscopic elastic properties of the medium (the slow time effects will be considered later in this paper). In general, the stress-strain dependence can be represented as [1, 2]

$$\sigma = M\varepsilon(1 + \Gamma_2\varepsilon + \Gamma_3\varepsilon^2 + \cdots) + \sigma_h(\varepsilon),$$
$$\sigma_h(\varepsilon) = \int_{-\infty}^{+\infty}\int_{0}^{+\infty} w(R, \xi)\tilde{\sigma}_h(\varepsilon, R, \xi)dRd\xi, \quad (5)$$

where σ_h is the part responsible for the hysteresis. This part should be found by integrating over the radii R of contacting grains and the pre-compressed indentation depths ξ (the latter are defined by the static force applied to each individual contact). The contacts of large curvature radii are associated with relatively large contact areas; these contacts remain near the main minimum. They are not involved in the attachment–detachment processes, but define the linear modulus and quadratic (cubic, etc.) nonlinearity. The contacts between asperities of smaller curvature radii can be attached and detached during cyclic deformation and thus are responsible for the hysteretic contribution. In the second equation (5), $w(R, \xi)$ is the probability density and $\tilde{\sigma}_h$ corresponds to elementary loops. Here, the normal distribution is assumed:

$$w(R, \xi) = \frac{\mathbb{N}}{w_{nrm}} \exp\left[-\frac{1}{2}\left(\frac{R - R_0}{\zeta_R}\right)^2\right] \times \exp\left[-\frac{1}{2}\left(\frac{\xi - \xi_0}{\zeta_\xi}\right)^2\right], \quad (6)$$

where $\mathbb{N}$ is the total number of adhesive contacts, $w_{nrm} = \pi\zeta_R\zeta_\xi\left[1 + \mathrm{erf}\left(\frac{R_0}{\zeta_R\sqrt{2}}\right)\right]$ is the normalizing factor, and R_0 and ξ_0 correspond to the mean values.

Figure 3 shows the result of integrating the individual dependences shown above in Fig. 2. Calculations were performed for $R_0 = 200$ μm and $\xi_0 = -2$ nm (static pre-compression). Standard deviation in the curvate radius was $\zeta_R = 70$ μm and standard deviation in ξ was varied: $\zeta_\xi = 0$ (line marked with circles), $\zeta_\xi =$

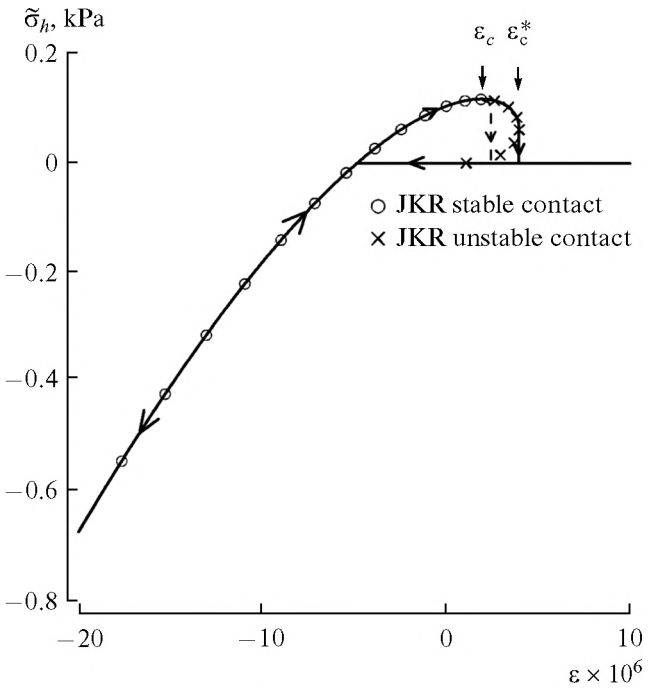

Fig. 2. Dependencies between normalized force and displacement according to (2) for quartz grains of R_g = 0.1 mm and contact curvature radius R = 1 mm. Crosses correspond to non-positive definite elastic energy [19].

0.5 nm (line marked with squares), and ζ_ξ = 10 nm (thick solid line). The latter curves are close to two parabolas, similar to most phenomenological models considered before (e.g., [1, 2]). From that, a linear dependence of the frequency shift and a quadratic dependence of the third harmonic on the strain amplitude, which have been observed in many experiments [1, 2], immediately follow.

The hysteresis effects in rocks are commonly observed after the strain amplitude exceeds a threshold value ε_0^*; according to [16], in sandstones $\varepsilon_0^* \approx (2–5) \times 10^{-7}$. The corresponding curvature radius R^* can be estimated from the bond strength (3) $|F_c^*| = 4\pi\sigma R_g^2$, where $\sigma = M\varepsilon_0^*$, and M is the experimental value from [16]. The resulting characteristic value is $R^* \approx 0.2$ μm, which corresponds to $\mu \sim 1$, as was expected. Although the JKR-model is, strictly speaking, not valid for $\mu \sim 1$, this estimation implies that the observed transition from a classical to hysteretic nonlinearity is explained by the activation of the contacts of relatively small curvature radii for which the adhesion hysteresis prevails, as was predicted by the proposed model.

SLOW-TIME RELAXATION

As was mentioned, at stronger strains with $\varepsilon_0 > \varepsilon_0^*$, the contacts between small asperities can be broken and then recovered; this process is responsible for the fast motion hysteresis. However, the smaller asperities irreversibly overcome the potential barrier shown on the upper panel of Fig. 1 and remain in the second, metastable minimum. The depth of the second minimum, $V_{\min}$ is much smaller than that of the primary one, and the corresponding equilibrium adhesion layer thickness h_m in (1) becomes larger. In this case, $\mu < 1$, so that the grains are not significantly deformed, whereas the adhesion layer thickness is varied without the hysteresis. These contacts return to the initial (main) state of equilibrium only due to the thermal

Materials studied were: (1) pearlite/graphite metal (gray iron), (2) alumina ceramic, (3) quartzite, (4) pyrex glass with cracks, (5) marble, (6) perovskite ceramic, (7) berea sandstone in air dry conditions, (8) berea sandstone in vacuum, (9) fontainebleau sandstone, (10) soil, (11) dry glass balls package, for brevity only scales are printed; small value corresponds to confining pressure 35 kPa, while the large one to 8 kPa. Data (1)–(6) are from [15], (7)–(9) from [14, 12], (10) from [17], and (11) from [18]

Material	M, GPa	Λ/M, $\times 10^{-5}$	Λ, MPa	V^*, 10^{-27} m^3	$d \equiv \sqrt[3]{V^*}$, nm
(1)	11.4	2.6–3.3	0.3–0.38	13–16	2.4–2.5
(2)	95	1.5	1.7	1.5	1.2
(3)	34	2.7	0.94	4.2	1.6
(4)	49.3	0.79	0.4	10	2.2
(5)	41.6	1.8	0.8	5.3	1.7
(6)	11.5	9.5	1.1	3.6	1.5
(7)	7.8	0.76	0.06	71	4.1
(8)	7.8	4.3	0.34	13	2.3
(9)	1.3	79	1	2.6	1.4
(10)	0.03	900	0.3	13	2.4
(11)	–	–	–	–	6–9

fluctuations; they are responsible for the slow time relaxation. To describe this process, we use an analogy with chemical reactions [28] and magnetic domain orientation [29, 30]. Namely, it is supposed that the strain recovery rate is governed by the Arrhenius law,

$$\dot{\varepsilon} = B\exp\left(-\frac{\Delta G}{kT}\right), \quad (7)$$

where B is a constant, ΔG is the Gibbs potential which has the order of the potential barrier in Fig. 1, k is the Boltzmann constant, and T is absolute temperature. It is possible to show that $\Delta G \gg kT$ for all the cases considered. In this case for a slow process with a small temperature change, the thermodynamic relation $-dG = V^*d\sigma + SdT \approx V^*d\sigma$, where V^* is "activation" volume associated with the relaxation process [29] and S is the entropy, is valid. As a result, Eq. (7) yields [17]

$$Md\varepsilon_s + \Lambda\frac{d\dot{\varepsilon}_s}{\dot{\varepsilon}_s} = d\sigma, \quad (8)$$

where subscript "s" is used for the slow processes occurring in excited states close to the metastable equilibrium, and $\Lambda = kT/V^*$.

If after the action of the load it is switched off at some moment $t = 0$ so that $\sigma(t \geq 0) = 0$, then the time dependence of the strain in (8) is logarithmic [17]:

$$\varepsilon_s = \varepsilon_s^{(0)} - \frac{\Lambda}{M}\ln\left(\frac{t+t_0}{t_0}\right), \quad (9)$$

where $\varepsilon_s^{(0)}$ is the initial strain and $t_0 = \dfrac{\Lambda}{M\dot{\varepsilon}_s^{(0)}}$. The initial strain value can be estimated as $\varepsilon_s^{(0)} = h_m/2R_g \sim 10^{-5}$, where $h_m \approx 2$–5 nm corresponds to the adhesion layer thickness at the second minimum (Fig. 1). The coefficient of the logarithm is determined from available experimental data (e.g., [12, 14, 15, 17, 18]). From there, the "activation" volume was then estimated as $V^* = kT/\Lambda$. The corresponding linear scale is estimated as $d = (V^*)^{1/3}$ and should be compatible with h_m for the second minimum (Fig. 1).

Table shows the main parameters of various materials tested in literature and the corresponding values of V^* and d calculated from the above relations. It is remarkable that very different materials are characterized by close "activation" scales, 1–4 nm. This suggests that the slow time phenomenon has a common cause in all these materials. Note that this scale is compatible with the second minimum's position in Fig. 1 and is of the order of a distance at which the surface force (4) effectively acts. Note also that the data in Table show the trend of increase in the activation scale with the structural/chemical inhomogeneity (materials 1, 4, 7, 8, and 10). Data no. 11 in table correspond to relaxation of bulk and shear elastic modulus of the air-dry glass balls package. Both values were found relaxed with the same rate and with the tendency of scale decrease with confining pressure increase. The characteristic d-values are greater because the intergrain forces are less in unconsolidated granular medium.

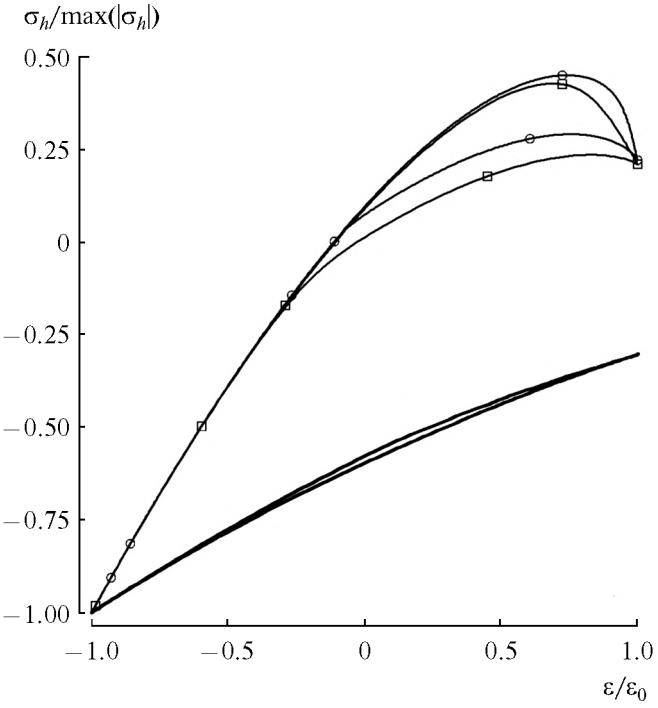

Fig. 3. Integral stress-strain curves plotted for a cyclic deformation amplitude $\varepsilon_0 = 10^{-5}$.

It is well-known [14] that upon relaxation the material returns to the same macroscopic state in which it was before the excitation at a high strain level, and this process is repeatable. This means that no irreversible changes takes place, as should be expected according to the model considered here. Experimental data [14] imply that relaxation phenomena occur when the excitation strain level exceeds ε_0^* value that corresponds to the transition from a classical to hysteretic nonlinearity. The latter was associated above with the asperities for which the parameter μ is large enough to provide hysteresis in the stress-strain dependence and the contacts attachment-detachment.

Reversibility of the relaxation process seems natural because only a small volumetric density of contacts, $\phi \ll 1$, can reach the metastable state. Strong bonds which are responsible for linear elasticity are not broken at all; correspondingly, the observed frequency shift in the fast motion hysteresis is only about 1%. The bulk of the material is not destroyed, but only weakly perturbed. The small discrepancy is eliminated in the course of relaxation due to thermal fluctuations, as discussed below.

As follows from most experiments (e.g., [14, 15]), the velocity and, correspondingly, resonant frequency of a weak probe wave propagating against the back-

ground of the main state slowly relaxing according to (9) also return logarithmically to their initial values. This readily follows from the expression for sound velocity which includes quadratic nonlinearity:

$$\frac{\Delta f}{f_0} = \frac{\Delta f_0}{f_0} + \frac{|\Gamma_2^e|\Lambda}{2M_0}\ln\left(\frac{t+t_0}{t_0}\right), \quad (10)$$

where f_0 is the unperturbed resonant frequency, $\Delta f_0 < 0$ is the initial frequency shift, and $\Gamma_2^e < 0$ is the effective quadratic nonlinearity coefficient averaged over all excited states. As follows from the above, $\Gamma_2^e \sim \Gamma_2\phi$; indeed, the averaged relaxing strain is of the order of $\phi\varepsilon_s$. This implies that the slope of the logarithmic relaxation function should be proportional to ϕ, as is seen from (10).

The strength of the grain contacts is proportional to the curvature radii. Therefore, it is reasonable to presume that the population density ϕ in the excited states is proportional to the excitation strain amplitude. Indeed, the logarithmic slope was observed to be linearly dependent on the excitation strain amplitude in [14]. Evidently, if $\varepsilon_0 < \varepsilon_0^*$, then no attachment-detachment process is activated, i.e., $\phi = 0$ and therefore no long-time relaxation occurs. These simple considerations can explain the bulk of observations (e.g., [2, 14, 15]) and provide an additional validation of the model proposed here.

RESULTS AND DISCUSSION

In this paper, apparently for the first time, a physical model of the nonlinear properties of structured media including geophysical materials, is proposed. It describes the classical elasticity, "fast" hysteresis, and the slow time relaxation within the framework of a unified description. The model is based on the contact potential containing a metastable minimum along with the main equilibrium, both occurring due to the contact adhesion forces together with the elastic forces acting between the grains. The model agrees with the main of experimental facts regarding the nonlinear resonance in bars and the slow time relaxation of a probe wave after a strong impact. A characteristic scale related to the relaxation process has been evaluated based on the experimental data; it is shown to amount to 1–4 nm for a variety of materials. Note that in our model, slow time behavior follows from the only fast of the existence of a secondary energy minimum, independently of any specific interaction mechanism causing this minimum.

It is proper to briefly outline other models known in the literature. In a series of papers (e.g., [31]) the hysteresis phenomenon is explained using a model accounting for the dry friction of rough surfaces in open cracks. Although the friction can play a significant role, the transition from a classical to hysteretic nonlinearity as well as the slow time phenomenon do not follow from the model. The slow time phenomenon was qualitatively described by the same authors in [32] within the framework of a model similar to [31]. It was assumed [32] that "due to thermally induced creep motion, the internal roughness may slowly vary in time." This assumption agrees with that proposed in [14]; however, the well-known fact of repeatability of the excitation-relaxation cycle pointed in [14] has not been explained.

Apparently, the first physical model of the slow-time relaxation phenomenon was described in [14]. The authors considered the excited state as that caused by the frictional slip during the fast motion at a moderate strain level. The relaxation is considered as recovery of the area of the microscopic contact due to the formation of bonds impeded by a smooth spectrum of energy barriers. Also, the question regarding repeatability of the fast-slow motion cycle remains. Nonetheless, this model leads to the relaxation with a logarithmic time dependence of sound velocity, and some results of [14] are still used in recent publications (e.g., [32]). Thus, let us compare the model proposed in the paper presented with [14]. The characteristic value of energy in the spectrum of energy barriers was estimated there as $E_{char} \approx 1.6 \times 10^{-7}$ pJ. In our estimates, the barrier height (Fig. 1, inset) is about 10^{-5}–10^{-4} pJ for a relatively large curvature radius, $R \sim 50$ nm, and the energy depends linearly on R. The value E_{char} in [14] corresponds to $R \sim 50$ nm when the parameter μ in (1) is small. Within the framework of the proposed theory, these contacts are not responsible for the adhesion hysteresis, whereas they can be associated with the slow time relaxation phenomena activated during the fast motion. Thus, the consideration of adhesive contact forces and compressibility of contact grains performed above allows describing both hysteresis and slow time effects uniformly based on prevalence of one over another at different stages of loading.

ACKNOWLEDGMENTS

The authors are grateful to P.A. Johnson for helpful discussions. The work was partly supported by the Russian Basic Research Foundation, projects no. 11-05-00774, 11-02-01419 and 13-05-97053, and Leading Scientific School project no. 5565-2014-2.

REFERENCES

1. L. A. Ostrovsky and P. A. Johnson, Riv. Nuovo Cimento, **24**, 1 (2001).
2. R.A. Guyer and P. A. Johnson, *Nonlinear Mesoscopic Elasticity: The Complex Behavior of Rocks, Soil, Concrete* (Wiley-VCH, 2009).
3. L. A. Ostrovsky, J. Acoust. Soc. Am. **116**, 3348 (2004).
4. A. V. Nazarov, A. V. Radostin, L. A. Ostrovsky, and I. A. Soustova, Acoust. Phys. **49**, 444 (2003).
5. V.E. Nazarov, Acoust. Phys. **57**, 192 (2011).

6. E. H. Field, P. A. Johnson, I. A. Beresnev, and Y. Zeng, Nature **390**, 599 (1994).
7. P. A. Johnson, P. Bodin, J. Gomberg, F. Pearce, Z. Lawrence, and F.-Y. Menq, J. Geophys. Res. **114**, B05304 (2009).
8. O. V. Rudenko, Giant nonlinearities in structurally inhomogeneous media and the fundamentals of nonlinear acoustic diagnostic techniques, Phys.-Usp. **49**, 69 (2006).
9. A. V. Lebedev, L. A. Ostrovsky, and A. M. Sutin, Akust. Zh. **51**, S88 (2005).
10. V. S. Averbakh, V. V. Artel'ny, B. N. Bogolyubov, V. V. Bredikhin, A. V. Lebedev, A. P. Maryshev, and V. I. Talanov, Acoust. Phys. **54**, 71 (2008).
11. V. Gusev and V. Tournat, Phys. Rev. B: Condens. Matter Mater. Phys. **72**, 05104 (2005).
12. J. A. TenCate and T. J. Shankland, Slow dynamics in the nonlinear elastic response of Berea sandstone, Geophys. Res. Lett. **23**, 3019 (1996).
13. K. W. Winkler and L. Xingzhou, J. Acoust. Soc. Am. **100**, 1392 (1996).
14. J. A. TenCate, E. Smith, and R. Guyer, Phys. Rev. Lett. **85**, 1020 (2000).
15. P. A. Johnson and A. M. Sutin, J. Acoust. Soc. Am. **117**, 124 (2005).
16. D. Pasqualini, K. Heitmann, J. A. TenCate, S. Habib, D. Higdon, and P. A. Johnson, J. Geophys. Res. **112**, B01204 (2007).
17. V. S. Averbakh, A. V. Lebedev, A. P. Maryshev, and V. I. Talanov, Acoust. Phys. **55**, 211 (2009).
18. V. S. Averbakh, A. V. Lebedev, S. A. Manakov, and V. V. Bredikhin, Radiophys. Quantum Electron. **56**, 135 (2013).
19. K. L. Johnson, K. Kendall, and A. D. Roberts, Proc. R. Soc. Lond. A **324**, 301 (1971).
20. J. N. Israelachvili, *Intermolecular and Surface Forces* (Academic, New York, 1992).
21. D. Maugis, J. Colloid Interface Sci. **150**, 243 (1992).
22. Y. L. Chen, C. A. Helm, and J. N. Israelachvili, J. Phys. Chem. **95**, 10736 (1991).
23. M. M. Sharma and A. N. Tutuncu, Geophys. Res. Lett. **21**, 2323 (1994).
24. V. A. Aleshin and K. Van Den Abeele, J. Mech. Phys. Solids **53**, 795 (2005).
25. K. Kendall, Energy analysis of adhesion, in *The Mechanics of Adhesion*, Ed. by D. A. Dillard and A. V. Pocius (Elsevier, New York, 2002), vol. 1, p. 77.
26. N. A. Burnham and A. J. Kulik, Surface forces and adhesion, in *Handbook of Micro/Nano Tribology*, Ed. by B. Bhushan (CRC, Boca Raton, 1999), 2nd ed., p. 263.
27. K. L. Page, Th. Proffen, S. E. McLain, T. W. Darling, and J. A. TenCate, Geophys. Res. Lett. **31**, L24606 (2004).
28. W. Stiller, *Arrhenius Equation and Non-Equilibrium Kinetics: 100 Years of Arrhenius Equation* (Teubner, Leipzig, 1989).
29. Y. Estrin, P. G. McCormic, and R. Street, J. Phys.: Condens. Matt. **1**, 4845 (1989).
30. J. A. TenCate, in *Proc. Int. Conf. on Nonlinear Elasticity in Materials* (Ticino, Switzerland, 2013), p. 84.
31. V. Aleshin and K. Van Den Abeele, J. Mech. Phys. Solids. **55**, 765 (2007).
32. V. Aleshin and K. Van Den Abeele, J. Mech. Phys. Solids. **55**, 366 (2007).